EXPERIMENTAL VALIDATION OF AN ADDITIVELY MANUFACTURED 1.3 GHz RADIO FREQUENCY CAVITY

H. Winter[*,†,1], V. Schuster[*,1], G. Dollinger[1], S. Brenner[1], V. Nedeljkovic-Groha[1], B. Reinarz[2], M. Mayerhofer[1]
[1]University of the Bundeswehr Munich, Neubiberg, Germany
[2]EOS GmbH Electro Optical Systems, Düsseldorf, Germany

Abstract

A compact continuous-wave (CW) 1.3 GHz linear particle accelerator (linac) is currently under development as the core component of a high energy positron annihilation lifetime spectroscopy setup. The associated thermal load imposes stringent requirements on the design and manufacturing of the underlying multi-cell radio-frequency (RF) cavity. Metal-based laser powder bed fusion (PBF-LB/M) has recently demonstrated the capability to fabricate pure copper RF cavities as monolithic components with integrated complex geometries, such as cooling channels. In this work, we present and evaluate a first 1.3 GHz single-cell RF cavity as a prototype for the intended multi-cell structure, manufactured from pure copper using PBF-LB/M. Helium leak rate and low-level RF measurements meet the linac expectations. While the dimensional accuracy is reduced compared to conventional manufacturing methods, it can be compensated by an iterative design approach. These results demonstrate, for the first time, the feasibility of PBF-LB/M as a manufacturing route for monolithic 1.3 GHz RF cavities.

INTRODUCTION

A 1.3 GHz linear particle accelerator (linac) is currently under development at the *University of the Bundeswehr Munich* for a novel material characterization setup based on pulsed positron annihilation lifetime spectroscopy [1]. The linac will accelerate positrons from a few keV up to 1 MeV in continuous-wave (CW) operation. To achieve a high shunt impedance and a compact layout, the linac design is based on a side-coupled radio-frequency (RF) cavity [2]. However, enabling CW operation and thus high positron count rates requires an advanced and highly integrated cooling system. Metal-based laser powder bed fusion (PBF-LB/M) enables the fabrication of highly complex normal-conducting RF cavities as monolithic components, allowing, in particular, enhanced cooling performance and reduced fabrication effort [3–9]. To date, the applicability of pure copper-based laser powder bed fusion (PBF-LB/Cu) to side-coupled RF cavities at 1.3 GHz has not yet been experimentally demonstrated. Therefore, in this work, we present and evaluate a PBF-LB/Cu-fabricated 1.3 GHz single-cell RF cavity (hereafter referred to as *cavity prototype*), representing the first accelerating cell of the planned side-coupled structure.

* These authors contributed equally to this work.
† Corresponding author: hermann.winter@unibw.de

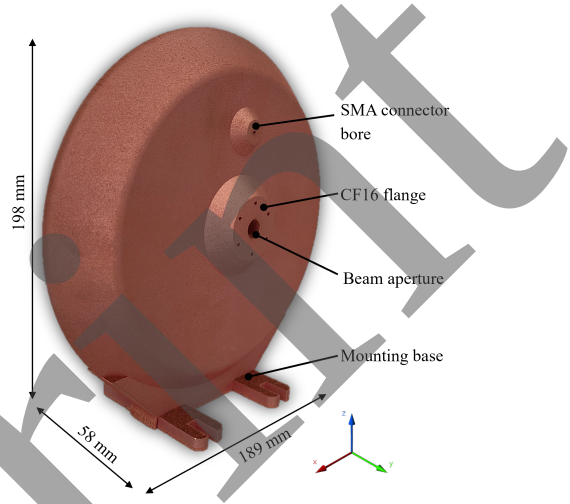

Figure 1: PBF-LB/Cu manufactured 1.3 GHz single-cell cavity structure with features.

MATERIALS AND METHODS

Figure 1 shows a picture of the manufactured cavity prototype, while Fig. 2(a) presents the corresponding CAD model. The cavity prototype was fabricated from pure copper (*EOS Copper CuCP* [10]) using an *EOS M290* [11] with a layer thickness of 40 µm and standard process parameters.

Each side of the cavity features a bore for mounting a *SubMiniature version A* (SMA) RF connector and a *ConFlat* (CF) 16 flange. The helium leak rate of the cavity prototype was evaluated using a *Pfeiffer ASM 340* helium leak detector [12] (Fig. 3). The CF16 flanges were CNC-machined to ensure proper sealing surfaces for elastomer O-rings. A plastic enclosure around the cavity ensured a saturated helium atmosphere during the measurement.

The resonance frequency f_R and unloaded quality factor Q_0 were measured using a *Siglent SNA5012A* vector network analyzer (VNA) [13] with capacitive input and output couplers, as shown in Fig. 4.

Dimensional accuracy was assessed using two complementary approaches. The deviation Δf_R between the simulated (*CST Studio Suite* [14]) and measured resonance frequency was used to evaluate the global geometric deviations [15]. Local geometric deviations were measured directly using a structured-light 3D scanner (*KEYENCE VL550* [16]) with a specified accuracy of 10 µm. The evaluated features are shown in Fig. 2(a).

In addition, metallographic microsections were analyzed at twelve locations across the cavity geometry to assess

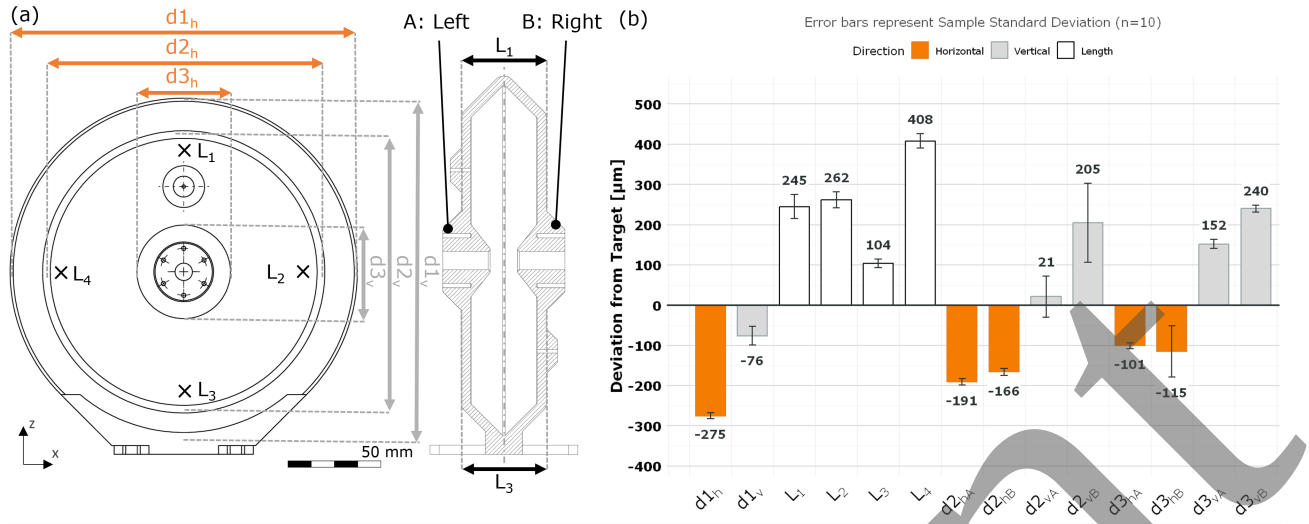

Figure 2: (a) CAD model of the cavity prototype including its measured geometric features. The features *d1*, *d2* and *d3* are measured in horizontal (h) and vertical (v) direction as well as on the left (A) and right (B) halves of the cavity. The feature *L* is measured at four locations (1, 2, 3, 4). (b) Deviation of the measured geometric features compared to the CAD file.

the relative material density. Figure 5 shows six representative microsections and their corresponding locations. The density was evaluated using a laser scanning microscope (*KEYENCE VK-X3000* [17]) in combination with *ImageJ* [18] software. The evaluated area per sample was 11 mm^2.

RESULTS AND DISCUSSION

Helium Leak Rate

The measurement setup is shown in Fig. 3, while the corresponding helium leak rate measurement is presented in Fig. 6. The maximum helium leak rate of less than 2×10^{-7} mbar L s^{-1} is reached after two hours. Scaled to the volume of the planned multi-cell cavity structure (length $\approx$ 1 m), an internal pressure of less than 4×10^{-8} mbar can be achieved using a standard turbomolecular pump with a pumping speed of 100 L s^{-1} [19]. This is considered sufficient for the intended application.

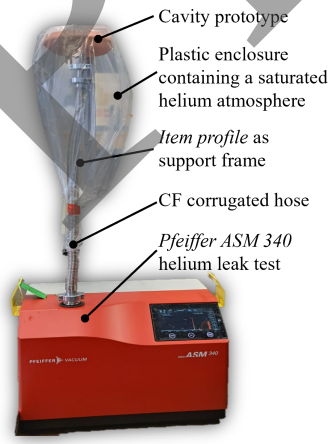

Figure 3: Helium leak rate test setup.

Furthermore, tests with localized helium exposure indicate that the measured integral leak rate is predominantly caused by the elastomer O-ring seals. Consequently, further improvements are expected when using metal sealing solutions, as demonstrated for PBF-LB/M cavities in [7].

Geometric Deviation

The measured geometric deviations and corresponding measurement locations are shown in Fig. 2. The averaged deviations of the planned diameter features (*d1, d2, d3*) are approximately -170 µm and +108 µm in horizontal (*h*) and vertical (*v*) direction, respectively. In horizontal direction, all diameter features are reduced compared to the CAD model, whereas in vertical direction four out of five features show an increase. The cavity length (*L*) is increased at all measurement positions (L_1 to L_4), with an average deviation of +178 µm. In addition, certain features exhibit a pronounced asymmetry between the left and right cavity halves (e.g. $d2_v$ and $d3_h$). The observed geometric deviations are most likely caused by PBF-LB/Cu-related thermal gradients and the resulting residual stresses during fabrication, leading to anisotropic shrinkage and distortion.

Low-Level RF Properties

The deviation Δf_R from the simulated resonance frequency is approximately 3.56 MHz. This can be attributed to the observed geometric deviations. To mitigate Δf_R, a geometry correction approach was investigated. By decreasing the cavity diameter by -176 µm (average of $d1_h$ and $d1_v$ and increasing the cavity length by +178 µm (average of L_1 to L_4), Δf_R could be reduced to approximately 1.78 MHz in simulations using *CST Studio Suite*. This corresponds to a reduction of about 50 % in Δf_R. These results demonstrate that simple geometric scaling can significantly improve frequency accuracy. In addition, established frequency tuning methods, such as elastic deformation or dimple tuning, are

expected to further reduce Δf_R by at least 1 MHz [20, 21]. It is therefore expected that the target resonance frequency f_R can be achieved by combining selective geometric compensation with an iterative manufacturing strategy.

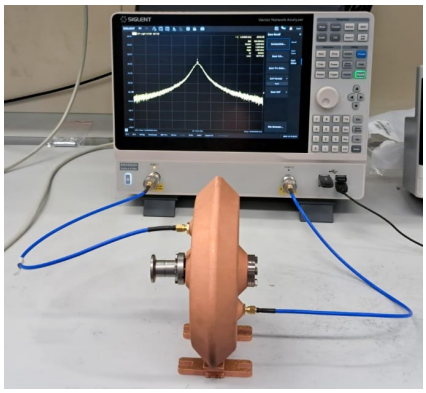

Figure 4: Measurement setup for low-level RF characteristics using a vector network analyzer.

The measured and simulated unloaded quality factors $Q_{0\mathrm{m}}$ and $Q_{0\mathrm{s}}$ are approximately 8600 and 14200, respectively. Taking into account the bulk electrical conductivity of copper ($\sigma_0 = 58\,\mathrm{MS\,m^{-1}}$) used in the simulation, the effective electrical conductivity of the cavity prototype can be estimated as $\sigma_{\mathrm{eff}} = \left(\frac{Q_{0\mathrm{m}}}{Q_{0\mathrm{s}}}\right)^2 \cdot \sigma_0 \approx 21\,\mathrm{MS\,m^{-1}}$. This corresponds to approximately 36 % of the International Annealed Copper Standard (IACS). However, due to the skin effect (skin depth $\delta \approx 1.8\,\mu\mathrm{m}$ at 1.3 GHz), the effective conductivity is predominantly governed by the intrinsically high surface roughness ($S_a > 10\,\mu\mathrm{m}$ [22]) of PBF-LB/Cu-manufactured surfaces. Therefore, post-processing steps are required to reduce surface roughness and improve Q_0. Chemical post-processing methods, such as Hirtisation® (*RENA Technologies Austria GmbH*), have been shown to increase Q_0 of PBF-LB/Cu cavities to values approaching 100 % of the simulated performance [3, 15].

Material Density

An average relative density of 99.88 % ± 0.09 % was determined from twelve microsections. Six representative micrographs are shown in Fig. 5. This further supports the assumption that the measured helium leak rate is dominated by the O-ring-based sealing concept rather than by the porosity of bulk material. Furthermore, the high material density indicates that the bulk electrical conductivity σ_0 is likely achieved, as reported for *EOS Copper CuCP* [10]. Consequently, the observed reduction in the quality factor Q_0 can be primarily attributed to surface roughness.

CONCLUSION

A 1.3 GHz cavity prototype was successfully fabricated using PBF-LB/Cu as a first demonstrator of a planned side-coupled multi-cell RF cavity. The measured helium leak rate meets the requirements of the intended application but is currently limited by the sealing concept. The measured

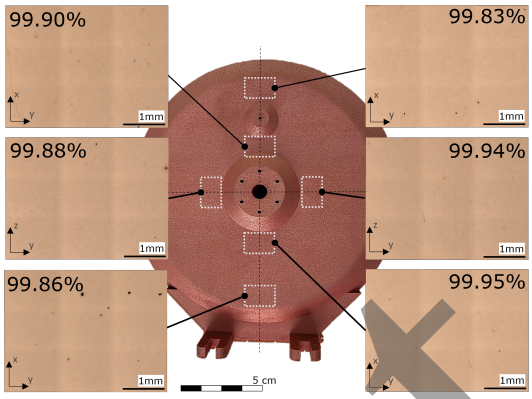

Figure 5: Metallographic microsections of the PBF-LB/Cu-fabricated cavity protoype.

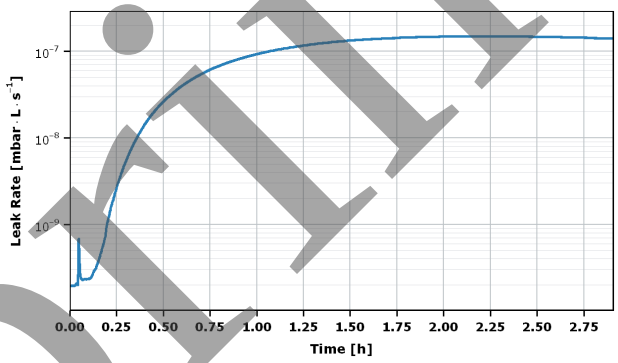

Figure 6: Measured helium leak rate.

unloaded quality factor Q_0 is reduced by approximately 60 % compared to the simulated value, consistent with previous studies. Post-processing is expected to increase Q_0 towards its theoretical limit. Geometric accuracy remains the main challenge, as process-induced deviations lead to a frequency shift of $\Delta f_R \approx 3.56$ MHz. However, pre-compensation of these deviations is expected to significantly reduce Δf_R. This work demonstrates, for the first time, the successful fabrication of a 1.3 GHz RF accelerator cavity using PBF-LB/Cu, highlighting the potential of this technology for this frequency regime. Future work will focus on PBF-LB/M-compatible design of the full multi-cell structure, detailed distortion analysis, and implementation of geometry compensation strategies.

ACKNOWLEDGEMENTS

This study is funded by the Federal Ministry of Research, Technology and Space (BMFTR) via the Project PosiLac (05K25WN1) and ERUM-Pro. In addition, the equipment used in this study, originating from the FLAB-3Dprint research project, is funded by dtec.bw—Research Center for Digitalization and Technology of the Bundeswehr. We would like to express our sincere gratitude for this support. dtec.bw is funded by the European Union—NextGenerationEU.

REFERENCES

[1] W. Egger *et al.*, "Pulsed low-energy positron beams: A useful tool to investigate defect structures in deformed metals and alloys," *J. Phys.: Conf. Ser.*, vol. 240, p. 012164, 2010. doi:10.1088/1742-6596/240/1/012164

[2] T. P. Wangler, *RF Linear Accelerators*, 2nd ed. Hoboken, NJ, USA: John Wiley & Sons, 2008.

[3] M. Mayerhofer *et al.*, "Additive manufacturing of side-coupled cavity linac structures from pure copper: A first concept," *Instruments*, vol. 7, no. 4, p. 56, 2023. doi:10.3390/instruments7040056

[4] T. Torims *et al.*, "First proof-of-concept prototype of an additive manufactured radio frequency quadrupole," *Instruments*, vol. 5, no. 4, p. 35, 2021. doi:10.3390/instruments5040035

[5] H. Hähnel *et al.*, "Additive manufacturing of an IH-type linac structure from stainless steel and pure copper," *Instruments*, vol. 7, no. 3, p. 22, 2023. doi:10.3390/instruments7030022

[6] H. Hähnel and U. Ratzinger, "First 3D printed IH-type linac structure—proof-of-concept for additive manufacturing of linac RF cavities," *Instruments*, vol. 6, no. 1, p. 9, 2022. doi:10.3390/instruments6010009

[7] S. Brenner *et al.*, "A radio-frequency quadrupole prototype additively manufactured as a multi-material component," *Prog. Addit. Manuf.*, vol. 10, pp. 3951–3961, 2025. doi:10.1007/s40964-025-01120-6

[8] T. Romano *et al.*, "Metal additive manufacturing for particle accelerator applications," *Phys. Rev. Accel. Beams*, vol. 27, p. 054801, 2024. doi:10.1103/PhysRevAccelBeams.27.054801

[9] C. Zhang *et al.*, "Development of a 704.4 MHz CH cavity using additive manufacturing," in *Proc. IPAC'23*, Venice, Italy, May 2023, pp. 1560–1563. doi:10.18429/JACoW-IPAC2023-TUPA185

[10] EOS GmbH, "EOS Copper CuCP material data sheet," 2026. https://www.eos.info/var/assets/05-datasheet-images/Assets_MDS_Metal/EOS_Copper_CuCP/Material_DataSheet_EOS_Copper_CuCP_en.pdf

[11] EOS GmbH, "EOS M 290 metal 3D printer data sheet," 2026. https://www.eos.info/metal-solutions/metal-printers/data-sheets/sds-eos-m-290

[12] Pfeiffer Vacuum GmbH, "ASM 340 helium leak detector – product leaflet," 2026. https://www.pfeiffer-vacuum.com/at/assets/112927/1/Product%20Leaflet%20ASM%20340%20Global%20EN.pdf

[13] Siglent Technologies Co., Ltd., "SNA5012A vector network analyzer," 2026. https://www.siglent.eu/product/5040548/siglent-sna5012a-9-khz-8-5-ghz-vector-network-analyzer

[14] Dassault Systèmes, "CST Studio Suite," 2026. https://www.3ds.com/products/simulia/cst-studio-suite

[15] M. Mayerhofer *et al.*, "Red and green laser powder bed fusion of pure copper in combination with chemical post-processing for RF cavity fabrication," *Instruments*, vol. 8, no. 3, p. 39, 2024. doi:10.3390/instruments8030039

[16] KEYENCE Corporation, "VL-500 series 3D scanner," 2026. https://www.keyence.de/products/3d-measure/3d-scanner/vl/models/vl-500/

[17] KEYENCE Corporation, "VK-X3000 laser scanning microscope," 2026. https://www.keyence.de/products/microscope/laser-microscope/vk-x3000/

[18] W. S. Rasband, "ImageJ," U.S. National Institutes of Health, Bethesda, MD, USA, 1997–2018. https://imagej.net/ij/

[19] Pfeiffer Vacuum GmbH, "HiPace 300 turbomolecular pump – product leaflet," 2026. https://www.pfeiffer-vacuum.com/global/assets/132737/1/Product%20Leaflet%20HiPace%20300%20P%20Global%20EN.pdf

[20] D. Ha *et al.*, "High precision tuning of RF cavity for 6 MeV SKKU X-band medical LINAC," *J. Korean Phys. Soc.*, vol. 85, pp. 591–599, 2024. doi:10.1007/s40042-024-01151-2

[21] A. Degiovanni, "High gradient proton linacs for medical applications," Ph.D. thesis, EPFL, Lausanne, Switzerland, 2014.

[22] R. Hu *et al.*, "Process of pure copper fabricated by selective laser melting technology under moderate laser power with re-melting strategy," *Materials*, vol. 16, no. 7, p. 2642, 2023. doi:10.3390/ma16072642